

Hybrid ultrasound and dual-wavelength optoacoustic biomicroscopy for functional neuroimaging

Johannes Rebling^{a,b}, Hector Estrada^a, Michael Zwack^b, Gali Sela^a, Sven Gottschalk^a, Daniel Razansky^{a,b}

^aInstitute for Biological and Medical Imaging (IBMI), Helmholtz Zentrum München, Neuherberg 85764, Germany;
^bTechnical University of Munich, Munich 81675, Germany;

ABSTRACT

Many neurological disorders are linked to abnormal activation or pathological alterations of the vasculature in the affected brain region. Obtaining simultaneous morphological and physiological information of neurovasculature is very challenging due to the acoustic distortions and intense light scattering by the skull and brain. In addition, the size of cerebral vasculature in murine brains spans an extended range from just a few microns up to about a millimeter, all to be recorded in 3D and over an area of several dozens of mm². Numerous imaging techniques exist that excel at characterizing certain aspects of this complex network but are only capable of providing information on a limited spatio-temporal scale. We present a hybrid ultrasound and dual-wavelength optoacoustic microscope, capable of rapid imaging of murine neurovasculature *in-vivo*, with high spatial resolution down to 12 μm over a large field of view exceeding 50mm². The dual wavelength imaging capability allows for the visualization of functional blood parameters through an intact skull while pulse-echo ultrasound biomicroscopy images are captured simultaneously by the same scan head. The flexible hybrid design in combination with fast high-resolution imaging in 3D holds promise for generating better insights into the architecture and function of the neurovascular system.

Keywords: neuroimaging, neurovasculature, cerebral vasculature, photoacoustic, brain imaging, multiwavelength

1. INTRODUCTION

A clear link exists between brain diseases related to cancer, stroke or Alzheimer's and the corresponding pathogenic alterations in the cerebral vasculature¹. However, the link between disease progression and vascular pathologies is often poorly understood due to the size and complexity of the brain's vascular network and the challenges imposed by *in-vivo* optical visualization of the highly scattering brain². Indeed, murine brain form highly complex vascular network with vessel size spanning a wide range of hundreds of microns down to just a few microns. The small capillaries are difficult to visualize *in vivo* using whole-body imaging techniques, such as magnetic resonance imaging³ and X-ray computed tomography⁴. On the other hand, optical microscopy methods, such as two-photon microscopy⁵ and optical coherence tomography⁶ offer the necessary micron-scale resolution, yet are limited in terms of the penetration depth, field-of-view and/or usable contrast for highly specific functional and molecular imaging.

Optoacoustic imaging (OA) with its combination of rich optical absorption contrast and ultrasound (US) depth penetration has matured tremendously over the last decade and has found widespread applications in biomedicine⁷⁻⁹. Optical-resolution OA microscopy (OR-OAM) has been employed for transcranial imaging of cerebral vasculature *in-vivo*¹⁰⁻¹² and was further successful in high-resolution visualization of other model organisms such as zebrafish¹³. However, the performance of the existing OR-OAM methods is impeded by limited field-of-view and depth of focus, thus necessitating prolonged scanning or tiling schemes to render meaningful 3D image volumes.

Here, we present a hybrid ultrasound and dual-wavelength optical-resolution optoacoustic microscope for functional neuroimaging *in-vivo*. The design is based on the previously introduced HFOAM system^{10,14} which was augmented for simultaneous ultrasonography and dual-wavelength optoacoustic imaging using a fast optical switch.

2. METHODS

The biomicroscope's design is illustrated in Fig. 1 and is based on the fast switching between a 532 nm Q-switched, diode end-pumped Nd:YAG laser (IS8II-E; EdgeWave GmbH, Würselen, Germany) and a dye laser (Credo, Sirah Lasertechnik GmbH, Grevenbroich, Germany) tuned to 578 nm. The wavelength switching is based on a Pockels cell (PC, Eksma Optics, Vilnius, Lithuania). When activated, the PC rotates the linear, s-polarized light of the diode laser light by 90° into a p-polarization. The subsequent polarizing beam splitter (PBS, Eksma Optics, Vilnius, Lithuania) then transmits the p-polarized light into the dye laser. When the PC is inactive, the polarization remains unchanged and the s-polarized diode laser light is reflected by the PBS. The PC can be switched at a pace of up to 10 kHz during the scan. Hence, the scan head is moving over the sample in a continuous manner while both the 532 nm and the 578 nm laser pulses and data acquisitions are triggered alternately.

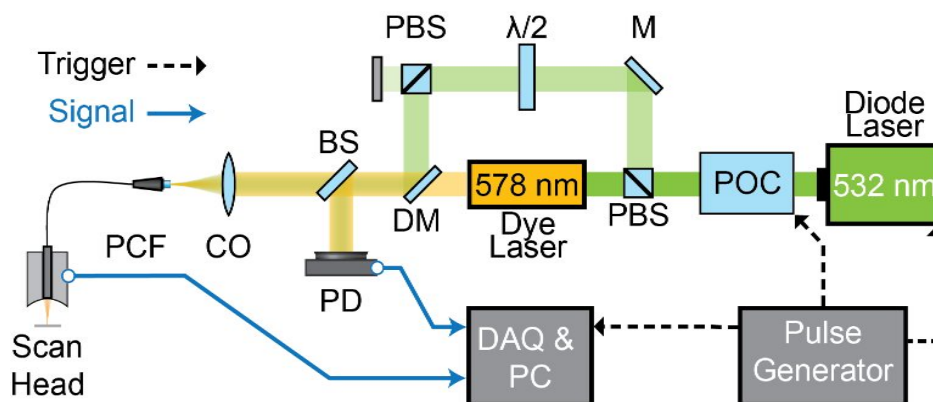


Figure 1. Illustration of the hybrid ultrasound and dual-wavelength optoacoustic biomicroscopy system. POC = Pockels cell, PBS – polarizing beam splitter, $\lambda/2$ – wave plate, DM – dichroic mirror, BS – beam sampler, CO – collimating lens, DAQ - data acquisition card, PD – photodiode.

Both the diode laser per pulse energy can be adjusted individually in order to exactly match the energies between both the diode and the dye laser. This is achieved using a combination of a rotating half-wave plate and an additional PBS (both Thorlabs, Newton, New Jersey, USA) in the diode laser beam path. The energy-matched beams are combined using a dichroic mirror (Thorlabs, Newton, New Jersey, USA) and coupled into a photonic crystal fiber. The fiber guides the light to a fast-moving scan head where both wavelengths are focused to a diffraction limited spot by means of a GRIN lens (Grintech GmbH, Jena, Germany). The GRIN lens is mounted through a central hole of a spherically focused US transducer (central frequency 30 MHz, Precision Acoustics, UK). The GRIN lens and the transducer are hence aligned coaxially and both the optical and the US foci are matched 7 mm away from the US transducer. The scan-head is then continuously scanned over the sample by means of a high-speed ultrasonic piezo linear stage (M-683, Physik Instrumente, Karlsruhe, Germany) and a DC motor driven linear stage (LTM 60F-25 HSM, OWIS GmbH, Staufen, Germany). For OA imaging, the lasers are triggered alternately and the generated OA signals are recorded by the US transducer and amplified by a preamplifier (Precision Acoustics, Dorchester, United Kingdom) and a 28 dB low-noise amplifier (ZFL-500LN, Mini-Circuits, New York, USA). Ultrasound imaging is performed in pulse-echo mode using a US pulser-receiver (5073PR, Olympus, Massachusetts, USA) and with the same US transducer and mechanical scanning. Both the amplified OA and US signals are digitized using a data acquisition card (M3i.4142, Spectrum Systementwicklung Microelectronic GmbH, Grosshansdorf, Germany) and stored on a PC. In order to characterize the optoacoustic resolution, a sharp edge of a Silicon piece (Fig. 2a) was scanned and the edge response was analyzed to determine the in-focus lateral resolution.

The 532 nm and 578 nm wavelengths are well suited for functional imaging due to the strong absorption contrast of blood in general and due to the spectral difference of oxy- and deoxyhemoglobin at those wavelengths. Both hemoglobin have a near identical absorption at the isosbestic point at 532 nm while the absorption of oxygenated hemoglobin is significantly stronger at 578 nm, which enables the measurement of the blood oxygen saturation^{12,15-17}. To test the system's capability for spectral differentiation, we imaged two tubes filled with red and blue ink (Pelikan, Hannover,

Germany) and formed a knot. Both inks have an identical absorption at 532 nm while the red ink has a much lower absorption at 578 nm, as measured with an optical spectrometer (not shown).

Next, a mouse brain was imaged *in-vivo* in order to extract both morphological and functional data of the complex cerebrovascular network. Six-week-old female athymic nude-Foxn1tm mice (Harlan Laboratories LTD, Itingen, Switzerland) were used for imaging, in full compliance with the institutional guidelines of the Helmholtz Center Munich and with approval from the Government District of Upper Bavaria. Animals were anesthetized with isoflurane (1.5% to 2.5% v/v) in 100% O₂. Physiological parameters, including blood oxygenation, heart rate, and body temperature were continuously monitored throughout the experiments. The temperature was kept constant using a rectal thermometer and a feedback-controlled heating pad (PhysioSuite, Kent Scientific, Torrington, CT, USA). A custom-designed stereotactic mouse head holder (Narishige International Limited, London, UK) was used to avoid animal motion. The mouse was imaged through the intact skull and with its scalp removed.

3. RESULTS AND DISCUSSION

Figure 2 displays the results of the lateral resolution characterization using a sharp silicon edge. Figure 2a) shows the used piece of silicon and indicates the imaged edge. A maximum intensity projection (MIP) of the volumetric OA data recorded at 532 nm is shown in Fig. 2b) with the corresponding resolution analysis along the x-direction displayed in Fig. 2c). Both the 532 nm and 578 nm (not shown) images have an in-focus resolution of 12 μm, as measured by the full-width at half maximum (FWHM) of the point spread function (PSF).

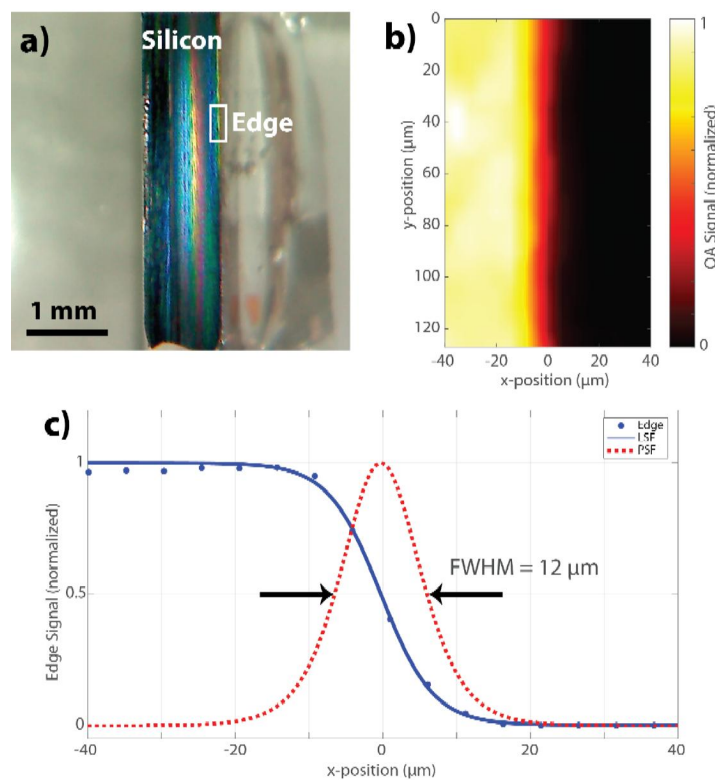


Figure 2. Optoacoustic resolution characterization of the system using a sharp silicon edge. a) Photo of the silicon piece, indicating the edge target. b) Maximum intensity projection of the silicon edge. c) Edge response (blue dots), fitted line-spread-function (LSF, blue solid line) and derived point-spread-function (PSF, red dashed line) showing the 12 μm lateral resolution.

The dual-wavelength imaging capability of the system is demonstrated in Fig. 3. Figures 3a) and b) show the recorded OA MIPs at 532 nm and 578 nm, respectively. In Fig. 3a) both ink-filled tubes are clearly visible and exhibit similar signal amplitudes, as is expected given their equal absorption. In contrast, only the tube filled with blue ink is visible in

Fig. 3b) due to the reduced absorption of the red ink at 578 nm. Using spectral unmixing, it is thus possible to measure and visualize the ink concentrations in the two knotted tubes, as shown in Fig. 3c).

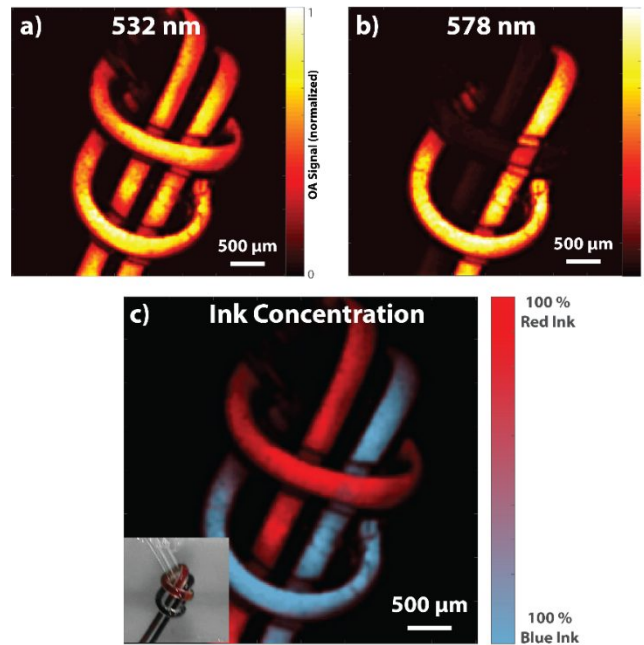


Figure 3. OA imaging of two ink-filled tubes forming a knot. a) and b) Optoacoustic maximum intensity projections recorded at 532 nm and 578 nm, respectively. The images in a) and b) are recorded simultaneously. c) Spectral unmixing of the OA data, providing the ink concentrations in the tubes.

Due to its hybrid nature, the newly introduced system can simultaneously image the entire skull and pial brain vasculature in both pulse-echo US and functional optoacoustic modes, as illustrated in Figure 4. Figure 4a) displays the pulse-echo US scan of the entire skull, while Fig. 4b) shows the corresponding brain vasculature imaged through the intact skull. Lastly, Fig. 4c) illustrates the measured blood oxygenation within the brain vasculature as measured via spectral unmixing of the OA data recorded at 532nm and 578 nm, respectively.

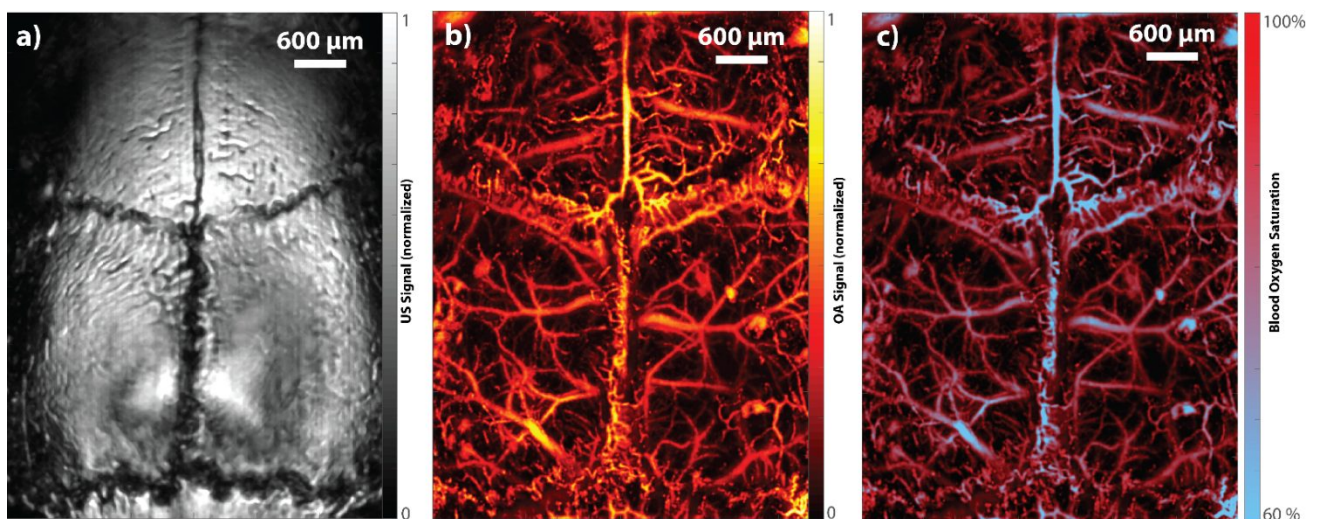


Figure 4. *In-vivo*, functional and large scale brain imaging of a murine model. a) Reflection-mode ultrasound image of the intact skull. b) Morphology of the brain imaged through the intact skull (optoacoustic maximum intensity projection of 3D image data). c) Functional imaging of the blood oxygenation based on the dual-wavelength optoacoustic data.

4. CONCLUSION

We have presented and characterized a novel hybrid ultrasound and dual-wavelength optoacoustic microscope and successfully applied this system to functional neuroimaging *in-vivo*. The system's lateral resolution has been characterized to be 12 μm for imaging at both 532 nm and 578 nm wavelengths. The spectral imaging capability has been showcased using ink-filled tube samples which allowed the examination of the ink concentration within the tubes. Lastly, the newly introduced system was applied for functional brain imaging, showcasing its ability to visualize both the large and complex cerebrovascular network in the murine brain as well as to measure its oxygen saturation *in-vivo*. The system therefore allows for a fast and high-resolution interrogation of the vascular morphology and function, facilitating investigations into the brain function in health and disease.

ACKNOWLEDGMENTS

This work was supported by the European Union through the OILTEBIA (Optical Imaging and Laser Techniques for Biomedical Applications) Grant (Agreement Number 317526) as well as by the European Research Council under grant agreement ERC-2015-CoG-682379. The authors declare no conflicts of interest.

REFERENCES

- [1] Klohs., Rudin., Shimshek., "Imaging of cerebrovascular pathology in animal models of Alzheimer's disease" (2014).
- [2] Insel, T., Landis, S., Collins, F., "The NIH BRAIN Initiative," 687–688 (2013).
- [3] Jonckers, E., Shah, D., Hamaide, J., Verhoye, M., Linden, A., "The power of using functional fMRI on small rodents to study brain pharmacology and disease," *Frontiers in pharmacology* **6** (2015).
- [4] Ghanavati., Lisa., Lerch., Sled., "A perfusion procedure for imaging of the mouse cerebral vasculature by X-ray micro-CT" (2014).
- [5] Weigert, R., Sramkova, M., Parente, L., Amornphimoltham, P., Masedunskas, A., "Intravital microscopy: a novel tool to study cell biology in living animals," *Histochem Cell Biol* **133**(5), 481–491 (2010).
- [6] Drexler, W., Liu, M., Kumar, A., "Optical coherence tomography today: speed, contrast, and multimodality," *Journal of Biomedical Optics* **19**(7), 071412, *Journal of Biomedical Optics* (2014).
- [7] Beard, P., "Biomedical photoacoustic imaging.," *Interface focus* **1**(4), 602–631 (2011).
- [8] Ntziachristos, V., Razansky, D., "Molecular Imaging by Means of Multispectral Optoacoustic Tomography (MSOT)," *Chemical Reviews* **110**(5), 2783–2794 (2010).
- [9] Taruttis., Ntziachristos., "Advances in real-time multispectral optoacoustic imaging and its applications" (2015).
- [10] Estrada, H., Turner, J., Kneipp, M., Razansky, D., "Real-time optoacoustic brain microscopy with hybrid optical and acoustic resolution," *Laser Physics Letters* **11**(4), 045601 (2014).
- [11] Kneipp, M., Turner, J., Estrada, H., Rebling, J., Shoham, S., Razansky, D., "Effects of the murine skull in optoacoustic brain microscopy.," *J Biophotonics* **9**(1-2), 117–123 (2016).
- [12] Zhang, H., Maslov, K., Sivaramakrishnan, M., Stoica, G., Wang, L., "Imaging of hemoglobin oxygen saturation variations in single vessels in vivo using photoacoustic microscopy," *Applied Physics Letters* **90**(5), 053901 (2007).
- [13] Kneipp, M., Estrada, H., Lauri, A., Turner, J., Ntziachristos, V., Westmeyer, G. G., Razansky, D., "Volumetric tracking of migratory melanophores during zebrafish development by optoacoustic microscopy.," *Mech. Dev.* **138 Pt 3**, 300–304 (2015).

- [14] Estrada, H., Sobol, E., Baum, O., Razansky, D., “Hybrid optoacoustic and ultrasound biomicroscopy monitors laser-induced tissue modifications and magnetite nanoparticle impregnation,” *Laser Physics Letters* **11**(12), 125601, *Laser Physics Letters* (2014).
- [15] Gottschalk, S., Fehm, T., Deán-Ben, X., Razansky, D., “Noninvasive real-time visualization of multiple cerebral hemodynamic parameters in whole mouse brains using five-dimensional optoacoustic tomography,” *Journal of cerebral blood flow and metabolism : official journal of the International Society of Cerebral Blood Flow and Metabolism* **35**(4), 531–535 (2015).
- [16] Laufer, J., Delpy, D., Elwell, C., Beard, P., “Quantitative spatially resolved measurement of tissue chromophore concentrations using photoacoustic spectroscopy: application to the measurement of blood oxygenation and haemoglobin concentration,” *Phys Med Biol* **52**(1), 141–168 (2006).
- [17] Yao, J., Wang, L., Yang, J.-M., Maslov, K., Wong, T., Li, L., Huang, C.-H., Zou, J., Wang, L., “High-speed label-free functional photoacoustic microscopy of mouse brain in action,” *Nature Methods* **12**(5), 407–410 (2015).